

Stellar laboratories (Research Note)

V. The Xe VI ultraviolet spectrum and the xenon abundance in the hot DO-type white dwarf RE 0503–289^{★, ★★}

T. Rauch¹, D. Hoyer¹, P. Quinet^{2,3}, M. Gallardo⁴, and M. Raineri⁴

¹ Institute for Astronomy and Astrophysics, Kepler Center for Astro and Particle Physics, Eberhard Karls University, Sand 1, 72076 Tübingen, Germany

e-mail: rauch@astro.uni-tuebingen.de

² Astrophysique et Spectroscopie, Université de Mons – UMONS, 7000 Mons, Belgium

³ IPNAS, Université de Liège, Sart Tilman, 4000 Liège, Belgium

⁴ Centro de Investigaciones Ópticas (CIOp), CC 3, 1897, Gonnet, La Plata, Argentina

Received 12 March 2015; 8 April accepted 2015

ABSTRACT

Context. For the spectral analysis of spectra of hot stars with a high resolution and high signal-to-noise ratio (S/N), advanced non-local thermodynamic equilibrium (NLTE) model atmospheres are mandatory. These are strongly dependent on the reliability of the atomic data that are used for their calculation.

Aims. Reliable Xe VI oscillator strengths are used to identify Xe lines in the ultraviolet spectrum of the DO-type white dwarf RE 0503–289 and to determine its photospheric Xe abundance.

Methods. We publish newly calculated oscillator strengths that are based on a recently measured Xe VI laboratory line spectrum. These strengths were used to consider their radiative and collisional bound-bound transitions in detail in our NLTE stellar-atmosphere models to analyze Xe VI lines exhibited in high-resolution and high S/N UV observations of RE 0503–289.

Results. We identify three hitherto unknown Xe VI lines in the ultraviolet spectrum of RE 0503–289 and confirm the previously measured photospheric Xe abundance of this white dwarf ($\log \text{Xe} = -4.2 \pm 0.6$ by mass).

Conclusions. Reliable measurements and calculations of atomic data are prerequisite for stellar-atmosphere modeling. Observed Xe VI line profiles in the ultraviolet spectrum of the white dwarf RE 0503–289 were well reproduced with the newly calculated Xe VI oscillator strengths.

Key words. atomic data – line: identification – stars: abundances – stars: atmospheres – stars: individual: RE 0503–289 – stars: white dwarfs

1. Introduction

Werner et al. (2012b) identified lines of ten trans-iron elements in the Far Ultraviolet Spectroscopic Explorer (FUSE¹) observations of RE 0503–289. They were only able to determine the photospheric krypton and xenon abundances because reliable transition probabilities were solely available for these species. New calculations of transition probabilities enabled us in the meantime to measure the abundances of Zn, Ge, Ga, and Ba (Rauch et al. 2014a, 2012, 2014b, 2015, respectively).

Recent measurements of Gallardo et al. (2015) have doubled the spectral information about Xe VI. Since reliable spectral analyses by means of non-local thermodynamic equilibrium (NLTE) model-atmosphere calculations need reliable transition probabilities for the complete model atom (and not only for the identified

lines), these new data allow improving the abundance determination of Xe. Moreover, the many newly classified Xe VI lines enable us to assign hitherto unidentified lines in the observation.

We start with an introduction to our observations and atmosphere models (Sects. 2 and 3). In Sect. 4, we briefly compare the new Xe VI transition probabilities to previous measurements. The line identification and abundance analysis is described in Sect. 5. We summarize the results in Sect. 6.

2. Observations

We analyzed the same FUSE spectrum ($910 \text{ \AA} < \lambda < 1188 \text{ \AA}$, resolving power $R = \lambda/\Delta\lambda \approx 20\,000$) that was previously described in detail by Werner et al. (2012b). In addition, we used our recently obtained (and later co-added) Hubble Space Telescope / Space Telescope Imaging Spectrograph (HST/STIS²) spectra (ObsIds OC7N01010, OC7N01020, grating E140M, $1144 \text{ \AA} < \lambda < 3073 \text{ \AA}$, $R \approx 45\,800$, 2014-08-14, total expo-

[★] Based on observations made with the NASA-CNES-CSA Far Ultraviolet Spectroscopic Explorer.

^{★★} Based on observations with the NASA/ESA Hubble Space Telescope, obtained at the Space Telescope Science Institute, which is operated by the Association of Universities for Research in Astronomy, Inc., under NASA contract NAS5-26666.

¹ <http://fuse.pha.jhu.edu>

² <http://www.stsci.edu/instruments/stis>

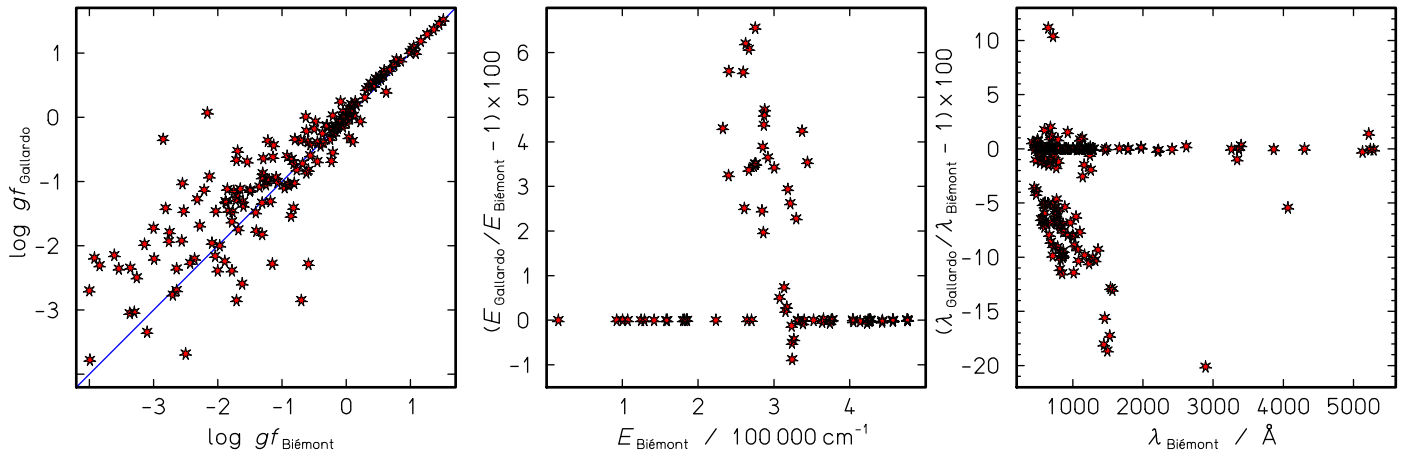


Fig. 1. Comparison of Xe VI data given by Biémont et al. (2005, B+05) and Gallardo et al. (2015, G+15). Left: weighted oscillator strengths ($\log gf$) in G+15 as a function of the B+05 values, middle: ratio of atomic level energies as a function of the B+05 values, right: ratio of line wavelengths as a function of the B+05 values.

sure time of 5494 s). The spectra are available via the Barbara A. Mikulski Archive for Space Telescopes (MAST³).

3. Model atmospheres

Our model atmospheres are plane-parallel, chemically homogeneous, and in hydrostatic and radiative equilibrium. They are calculated with the Tübingen NLTE Model Atmosphere Package (TMAP⁴, Werner et al. 2003, 2012a). Model atoms were constructed from the Tübingen Model Atom Database (TMAD⁵, Rauch & Deetjen 2003). TMAD has been constructed as part of the Tübingen contribution to the German Astrophysical Virtual Observatory (GAVO⁶).

4. Xe VI transition probabilities

For their analysis of RE 0503–289, Werner et al. (2012b) used Xe VI data of Reyna Almandos et al. (2001), who used the Hartree-Fock relativistic (HFR) approach to calculate weighted oscillator strengths (gf) of 104 spectral lines belonging to the $5s5p^2$, $5s^25d$, $5s^26s$, $5s5p5d$, $5p^3$, and $5s5p6s$ transitions array. In addition, gf -values of an experimental and theoretical study Biémont et al. (2005) were used. These replaced gf -values of Reyna Almandos et al. (2001) where available. They were calculated for $\Delta n = 0$ and $\Delta n = 1$ transitions connecting the $5s^2nl$ [np (n=5-8); nf (n=4-5); nh (n=6-8); nk (n=8)], $5s5pnl$ (nl=5d,6s), $5p^3$, $5s^2nl$ [ns (n=6-8); nd (n=5-8); ng (n=5-6); ni (n=7-8)], and $5s5p^2$ configurations. Core-polarization (CP) effects were included in their HFR approach. Good agreement was observed between theory and experiment.

Gallardo et al. (2015) observed 243 lines (146 classified for the first time) of the Xe VI spectrum within $400 \text{ Å} \leq \lambda \leq 5500 \text{ Å}$. They calculated gf -values of $5s5p5d$ and $5s5p6s$ configurations. Biémont et al. (2005) encountered a problem in matching the 6d experimental level in their least-squares calculations, which Gallardo et al. (2015, see this paper for further technical details) solved by adjusting configuration interaction (CI) integrals. They achieved standard deviations of 149 cm^{-1} in the odd parity

energies (35 configurations) and 154 cm^{-1} (34 configurations) in the even parity.

We updated our Xe VI model ion (Werner et al. 2012b) with their experimental level energies (88 levels, 32 classified for the first time, 33 with revised energies) and oscillator strengths (used in the formulae for the cross-sections of radiative and collisional bound-bound transitions). The new Xe VI model ion is available via TMAD.

Figure 1 shows the comparison of the Xe VI $\log gf$ values, level energies, and line wavelengths of Biémont et al. (2005) and the Gallardo et al. (2015). For the strongest lines, that is, $\log gf > 0.0$, the agreement of the oscillator strengths is very good. The energy levels deviate significantly in the $230\,000 \text{ cm}^{-1} < E < 350\,000 \text{ cm}^{-1}$ interval. This results in stronger differences of the lines' wavelengths in the ultraviolet wavelength range ($\lambda < 1700 \text{ Å}$). The following comparison will verify the quality of the new data.

We start reproducing the lines shown by Werner et al. (2012b). Table 1 shows a comparison of the $\log gf$ values that they used with the new values.

Figure 2 demonstrates how the new oscillator strengths influence the line-profile fits. Because of their much higher $\log gf$ values, Xe VI $\lambda\lambda 928.366, 1101.947 \text{ Å}$ now match the observation significantly better, while the other lines are almost unchanged. The Xe VII lines are too strong, most likely as a result of our insufficient Xe VII model ion, for which only two oscillator strengths are known (namely of these two lines). In Sect. 5, we search in the FUSE and HST/STIS spectra for further Xe VI lines to evaluate the oscillator strengths.

5. Line identification and abundance determination

We compared our best model spectra with our FUSE and STIS observations to identify additional Xe VI lines. We found only a few (Fig. 3). Xe VI $\lambda\lambda 929.121, 1017, 270 \text{ Å}$ have apparently blends with so far unknown lines. Xe VI $\lambda 1298.910 \text{ Å}$ matches the STIS observation well. Since all observed Xe lines are reproduced well, we confirm the abundance determination by Werner et al. (2012b, $\log \text{Xe} = -4.2 \pm 0.6$). The two identified Xe VII $\lambda\lambda 995.511, 1077.12 \text{ Å}$ lines (oscillator strengths from Kernahan et al. 1980; Biémont et al. 2007, respectively) are stronger than observed at this abundance (hence the relatively broad error range), but this may be an artifact due to the lack of

³ <http://archive.stsci.edu/>

⁴ <http://astro.uni-tuebingen.de/~TMAP>

⁵ <http://astro.uni-tuebingen.de/~TMAD>

⁶ <http://www.g-vo.org>

Table 1. Comparison of the $\log gf$ values of Xe VI lines calculated by Biémont et al. (2005) and used by Werner et al. (2012b) with those calculated by Gallardo et al. (2015).

transition	$\lambda / \text{\AA}$	$\log gf$	
		Biémont	Gallardo
$5s5p^2 \ ^2D_{3/2} - 5p^3 \ ^2D_{3/2}^o$	928.37	-2.11	-0.649
$5s5p^2 \ ^2D_{5/2} - 5p^3 \ ^2D_{3/2}^o$	967.55	-1.14	-0.937
$5s^25p \ ^2P_{1/2}^o - 5s5p^2 \ ^4P_{3/2}$	996.23	-3.37	-3.049
$5s^25p \ ^2P_{1/2}^o - 5s5p^2 \ ^4P_{1/2}$	1080.08	-1.64	-1.529
$5s^25p \ ^2P_{3/2}^o - 5s5p^2 \ ^4P_{5/2}$	1091.63	-1.25	-1.045
$5s5p^2 \ ^2P_{1/2} - 5p^3 \ ^2D_{3/2}^o$	1101.95	-2.13	-0.606
$5s^25d \ ^2D_{5/2} - 5s^26p \ ^2P_{3/2}^o$	1136.41	+0.06	-0.005
$5s^25p \ ^2P_{3/2}^o - 5s5p^2 \ ^4P_{3/2}$	1179.54	-2.09	-1.958
$5s^25d \ ^2D_{3/2} - 5s^26p \ ^2P_{1/2}^o$	1181.46	-0.21	-0.226

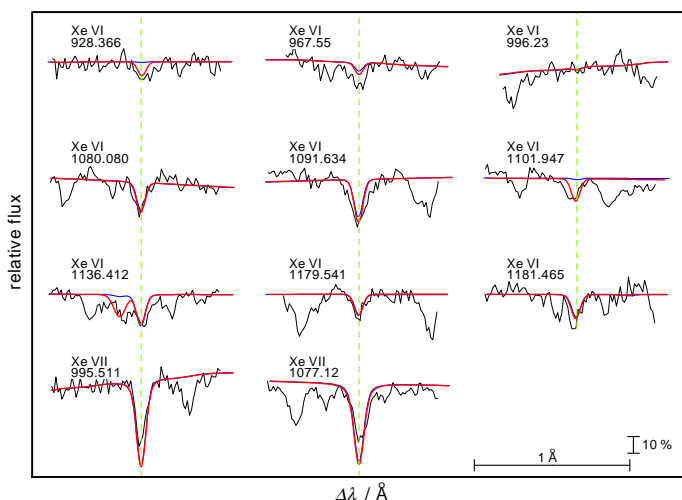


Fig. 2. Xe VI and Xe VII lines calculated from TMAP model atmospheres with $T_{\text{eff}} = 70\,000\text{ K}$, $\log g = 7.5$, and $\log \text{Xe} = -4.2$ (mass fraction) compared with the FUSE observation. Thin (blue in the online version): model of Werner et al. (2012b, N IV λ 1136.27 \AA was not included in the calculation), thick (red) our model. The vertical bar indicates 10% of the continuum flux level.

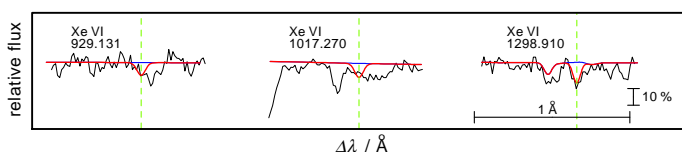


Fig. 3. Xe VI lines calculated from the same models as in Fig. 2 compared with the FUSE and STIS (right panel, Ni V λ 1298.738 \AA appears left of Xe VII λ 1298.910 \AA) observations. Thin (blue in the online version): model without Xe, thick (red) model including Xe.

reliable Xe VII oscillator strengths, cf. Werner et al. (2012b, see Sect. 1 above).

6. Results and conclusions

The recently presented oscillator strengths of Gallardo et al. (2015, 243 lines) complement and improve available data of Reyna Almandos et al. (2001, 104 lines) and Biémont et al. (2005, 491 lines). A comparison of data for lines that are listed in Gallardo et al. (2015) and Biémont et al. (2005) showed that

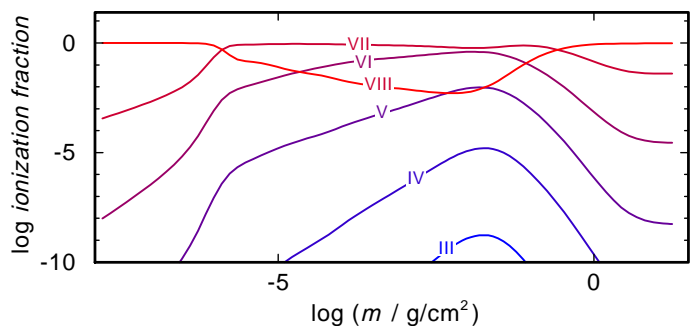


Fig. 4. Xe VI ionization fractions in our best model for RE 0503–289 (Rauch et al. 2015).

the $\log gf$ values agree well for the strongest lines. Deviations in the line wavelengths are noted, but they do not affect the identified lines in the UV spectra of RE 0503–289 and cannot be assessed. However, a comprehensive recalculation of Xe VI transition probabilities is desirable.

The oscillator strengths of Gallardo et al. (2015) significantly improve the agreement of the synthetic Xe VI line profiles with the observations in two of nine cases. The abundance determination of Werner et al. (2012b, $\log \text{Xe} = -4.2 \pm 0.6$) was confirmed.

Figure 4 shows that Xe VII is the dominant Xe ionization stage in the in the line-forming region ($-4 \lesssim \log m \lesssim 0.5$). m is the mass column density, measured from the outer limit of the atmosphere. Therefore, we expect to identify many more Xe VII lines once reliable oscillator strengths for the complete Xe VII model ion are available. This is mandatory to be able to reduce the uncertainty in the Xe abundance analysis.

Acknowledgements. TR and DH are supported by the German Aerospace Center (DLR, grants 05 OR 1402 and 50 OR 1501, respectively). The GAVO project at Tübingen had been supported by the Federal Ministry of Education and Research (BMBF, grants 05 AC 6 VTB, 05 AC 11 VTB). Financial support from the Belgian FRS-FNRS is also acknowledged. PQ is research director of this organization. Some of the data presented in this paper were obtained from the Mikulski Archive for Space Telescopes (MAST). STScI is operated by the Association of Universities for Research in Astronomy, Inc., under NASA contract NASS-26555. Support for MAST for non-HST data is provided by the NASA Office of Space Science via grant NNX09AF08G and by other grants and contracts. This research has made use of NASA’s Astrophysics Data System and the SIMBAD database, operated at CDS, Strasbourg, France.

References

- Biémont, É., Buchard, V., Garnir, H.-P., Lefèbvre, P.-H., & Quinet, P. 2005, *European Physical Journal D*, 33, 181
- Biémont, É., Clar, M., Fivet, V., et al. 2007, *European Physical Journal D*, 44, 23
- Gallardo, M., Raineri, M., Reyna Almandos, J., Pagan, C. J. B., & Abrahão, R. A. 2015, *ApJS*, 216, 11
- Kernahan, J. A., Pinnington, E. H., O’Neill, J. A., Bahr, J. L., & Donnelly, K. E. 1980, *Journal of the Optical Society of America (1917-1983)*, 70, 1126
- Rauch, T. & Deetjen, J. L. 2003, in *Astronomical Society of the Pacific Conference Series*, Vol. 288, *Stellar Atmosphere Modeling*, ed. I. Hubeny, D. Mihalas, & K. Werner, 103
- Rauch, T., Werner, K., Biémont, É., Quinet, P., & Kruk, J. W. 2012, *A&A*, 546, A55
- Rauch, T., Werner, K., Quinet, P., & Kruk, J. W. 2014a, *A&A*, 564, A41
- Rauch, T., Werner, K., Quinet, P., & Kruk, J. W. 2014b, *A&A*, 566, A10
- Rauch, T., Werner, K., Quinet, P., & Kruk, J. W. 2015, *ArXiv* 1501.07751
- Reyna Almandos, J., Sarmiento, R., Raineri, M., Bredice, F., & Gallardo, M. 2001, *J. Quant. Spec. Radiat. Transf.*, 70, 189
- Werner, K., Deetjen, J. L., Dreizler, S., et al. 2003, in *Astronomical Society of the Pacific Conference Series*, Vol. 288, *Stellar Atmosphere Modeling*, ed. I. Hubeny, D. Mihalas, & K. Werner, 31
- Werner, K., Dreizler, S., & Rauch, T. 2012a, TMAP: Tübingen NLTE Model-Atmosphere Package, *Astrophysics Source Code Library*
- Werner, K., Rauch, T., Ringat, E., & Kruk, J. W. 2012b, *ApJ*, 753, L7